

ON THE DEVELOPMENT OF A LOW PEAK-POWER, HIGH REPETITION-RATE LASER PLASMA ACCELERATOR AT IPEN*

A. Bonatto[†], Universidade Federal de Ciências da Saúde de Porto Alegre, Porto Alegre, Brazil
E. P. Maldonado, Instituto Tecnológico de Aeronáutica (ITA), São José dos Campos, Brazil
R. P. Nunes, Universidade Federal do Rio Grande do Sul, Porto Alegre, Brazil
A. V. F. Zuffi, F. B. D. Tabacow, R. E. Samad, N. D. Vieira, Instituto de Pesquisas Nucleares e Energéticas (IPEN/CNEN), São Paulo, Brazil

Abstract

In this work, the current status on the development of a laser plasma accelerator at the Nuclear and Energy Research Institute (Instituto de Pesquisas Nucleares e Energéticas, IPEN/CNEN), in São Paulo, Brazil, is presented. Short pulses to be produced by an under-development near-TW, kHz laser system will be used to ionize a gas jet, with a density profile designed to optimize the self-injection of plasma electrons. The same laser pulse will also drive a plasma wakefield, which will allow for electron acceleration in the self-modulated regime. The current milestone is to develop the experimental setup, including electron beam and plasma diagnostics, required to produce electron bunches with energies of a few MeV. Once this has been achieved, the next milestone is to produce beams with energies higher than 50 MeV. Besides kickstarting the laser wakefield accelerator (LWFA) technology in Brazil, this project aims to pave the way for conducting research on the production of radioisotopes by photonuclear reactions, triggered by LWFA-accelerated beams.

INTRODUCTION

Since laser wakefield accelerators (LWFA) were conceptually proposed [1], laser technology has significantly evolved [2–4]. State-of-the-art LWFA facilities can now produce high-quality, multi-GeV electron beams [5], by utilizing gas-filled capillaries to guide ultrashort, near-PW laser pulses within a few tens of centimeters. However, the low-repetition-rate operation due to the demanding laser-system requirements, as well as the complexity added by the capillary target, prevent the wide adoption of such setup for applications. Studies on high-repetition-rate operation in the self-modulated regime (SM-LWFA) [6, 7] show that this alternative might help bridging the gap between LWFA development and application. Despite the lower energy and quality, beams with higher charge can be obtained in the SM-LWFA, if compared to those produced in the non-linear or bubble regime [6]. The less-demanding laser requirements (longer pulses, with lower peak power), and the production of beams with higher charge [6, 8] at \sim kHz frequencies, combined with the lower complexity of using gas jets rather than capillaries, are attractive reasons for revisiting the SM-LWFA with modern laser systems. In this work, the status

of the ongoing development of a SM-LWFA at IPEN is presented. In addition, preliminary estimates from PIC simulations show that the goal of the current phase, which is producing electron beams with energies of a few MeV, is attainable with the proposed setup.

STATUS OF THE EXPERIMENTAL SETUP

Experiments are performed at IPEN with laser pulses produced by a hybrid Ti:Sapphire/Cr:LiSAF CPA system. The CPA frontend is a Quantronix Odin laser that generates \sim 50 fs, 1 mJ pulses at 1 kHz. The system has been modified to allow for the extraction of the amplified, uncompressed pulses, which are then sent to a in-house, custom-designed Cr:LiSAF multipass amplifier [9, 10] and compressor, generating up to 0.5 TW pulses at 5Hz. These systems are shown in Fig. 1. Currently, we are upgrading the system, replacing the Cr:LiSAF by a multipass Ti:sapphire amplifier, aiming to obtain near-TW pulses at higher repetition rates.

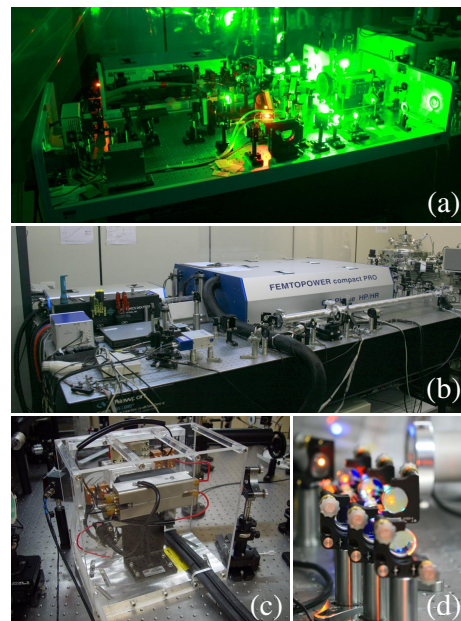


Figure 1: Laser systems available at the Center for Laser and Applications. (a) Quantronix Odin Ti:Sapphire ($E_p \leq 1$ mJ, $f \leq 1$ kHz, $\tau \approx 50$ fs); (b) Femtopower Ti:Sapphire ($E_p \leq 800$ μ J, $f \leq 4$ kHz, $\tau \approx 25$ fs); (c) in-house built, lamp-pumped Cr:LiSAF amplifier (0.5 TW at 5 Hz); (d) hollow fiber compressor ($E_p \leq 350$ μ J, $f \leq 4$ kHz, $\tau < 6$ fs, 50-attosecond CEP stabilized).

* Work supported by FAPESP, CNPq, and CAPES.

[†] abonatto@ufcsa.edu.br

Content from this work may be used under the terms of the CC BY 3.0 licence (© 2021). Any distribution of this work must maintain attribution to the author(s), title of the work, publisher, and DOI

For the target area, the vacuum chamber shown in Fig. 2 will accommodate in-house designed and manufactured de Laval supersonic gas jets [11–13]. As shown in Fig. 3, computational fluid dynamics is used to evaluate the gas density and Mach number distributions for distinct submillimeter nozzle specifications. Figure 4 shows that, by changing the ultrashort pulse laser drilling process from percussion to trepanning, both roundness and roughness were greatly improved. As a consequence, the gas flow properties might be improved as well.

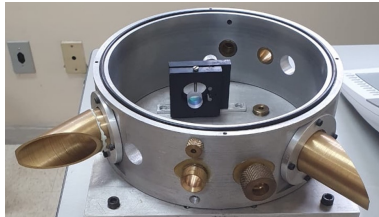


Figure 2: Vacuum chamber.

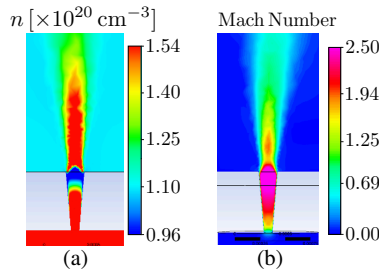


Figure 3: Supersonic gas jets are designed with aid of computational fluid dynamics simulations for the (a) gas density, and (b) Mach number distribution.

Regarding density diagnostics, a modified Mach-Zehnder interferometer with ultra-short pulses is being employed to characterize the density profile of gas targets and laser-ionized plasmas, in both space and time [14]. Figure 5(a) shows the phase-shift accumulated by the interferometer laser beam propagating through a gas jet. This phase-shift map – which is extracted from an interferogram – can be used to determine the gas density distribution. While a continuously flowing gas target can be diagnosed by continuous-wave (CW) interferometry, pump-probe techniques are needed to analyze a laser-excited plasma. Due to the short plasma-formation time and excited-ions fast decay, the signal would fade out in CW techniques due to the exceedingly small duty-cycle. Figure 5(b) shows plasma-density maps measured at 150 ps and 450 ps after the plasma creation by focused ultrashort pulses.

NUMERICAL SIMULATIONS

Particle-in-cell (PIC) simulations were performed by using FBPIC code [15], for the matched propagation (in a transverse parabolic channel [6]) of a Gaussian laser pulse in the longitudinal plasma-density profile shown in Fig. 6. Figure 7 show results from a parameter scan for laser pulses

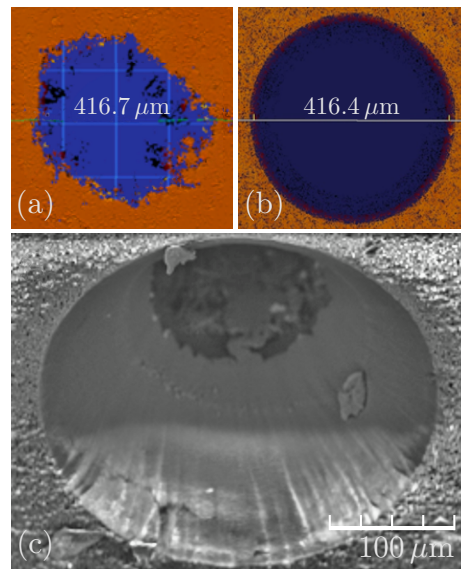


Figure 4: De Laval nozzle manufacturing process has been improved. (a) Laser percussion drilling (150 μJ pulses) in a copper plate was replaced by (b) trepanning on an alumina disk. (c) Besides the much improved roundness, scanning electron micrography shows that the residual roughness on the trepanned surface is lower than that on the alumina surface.

with peak power ranging from 0.25 TW to 1 TW, and plasma densities within $0.5 \sim 10 \times 10^{20} \text{ cm}^{-3}$. While panel (a) shows the beam total charge Q_T , panels (b) and (c) show the median and maximum kinetic energy, \tilde{K} and K_{max} , respectively. Figure 8 shows simulation results for a laser pulse with peak power $P_\ell = 1 \text{ TW}$, RMS length $\sigma_\ell = 15 \mu\text{m}$ and waist $w_0 = 7 \mu\text{m}$ (laser strength parameter $a_0 = 0.78$), propagating in a

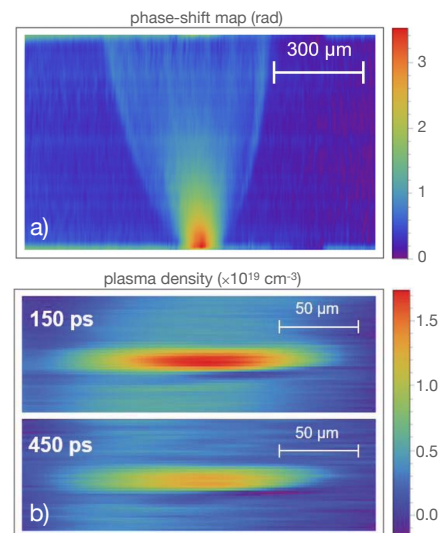


Figure 5: (a) Phase-shift map of the gas flow into $\sim 100 \text{ mbar}$ background pressure and 50 bar of N_2 backing pressure. (b) Plasma-density maps (in atmosphere) for 150 ps and 450 ps after its formation.

plasma with density $n_0 \approx 2.8 \times 10^{20} \text{cm}^{-3}$, with longitudinal profile as shown in Fig. 6, and transverse homogeneous profile. Panel (a) shows Q_{sel} , the charge of electrons with kinetic energies $E_k \geq E_{k,min}$, with $E_{k,min}$ ranging from 1 MeV to 5 MeV, plotted as a function of the pulse propagation distance $s \equiv z_0 + ct$, where $z_0 = -50 \mu\text{m}$. Panel (b) depicts the energy spectrum for electrons with $E_k \geq 1 \text{ MeV}$, plotted after these particles have exited the plasma density-profile.

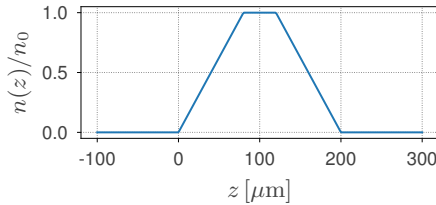


Figure 6: Longitudinal plasma-density profile. Transversely, the plasma is homogeneous.

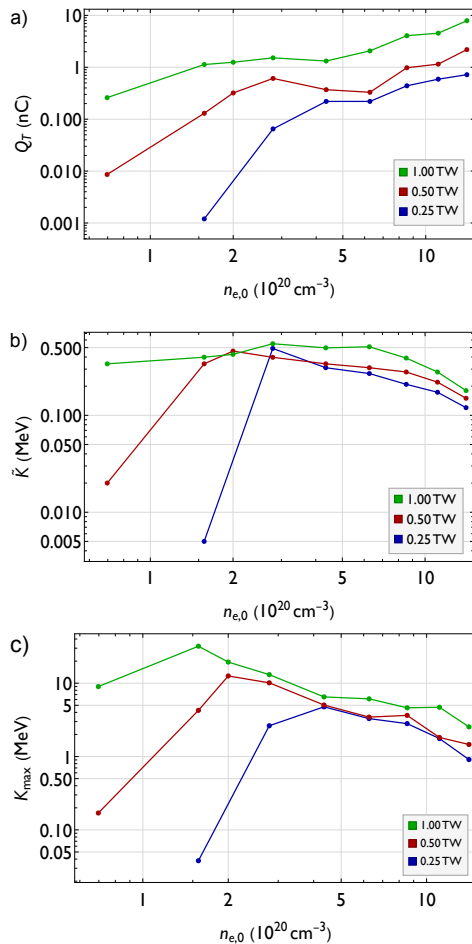


Figure 7: (a) Beam total charge, and (b) median and (c) maximum kinetic energy obtained from multiple PIC simulations, performed for laser pulses with peak power ranging from 0.25 TW to 1 TW, and plasma densities within $0.5 \sim 10 \times 10^{20} \text{cm}^{-3}$.

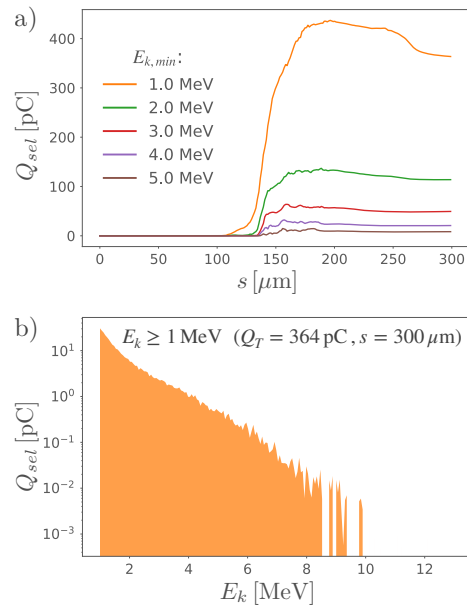


Figure 8: (a) Q_{sel} , the charge of electrons with kinetic energies $E_k \geq E_{k,min}$, plotted as a function of s ; (b) energy spectrum for electrons with $E_k \geq 1 \text{ MeV}$, plotted at $s=300 \mu\text{m}$.

CONCLUSION

In this work, the current status of the ongoing SM-LWFA development at IPEN was presented. Advances were made in the gas nozzle designing and manufacturing, and initial measurements of the gas and plasma density are being checked/validated. In addition, preliminary simulations corroborated the feasibility of achieving energies of a few MeV for the proposed setup. Through a collaboration with the University of Nebraska-Lincoln, the proposed setup will be experimentally verified with gas nozzles manufactured at IPEN. After the laser-system upgrade, such experiments will be performed at IPEN. Regarding studying the production of ^{99}Mo via photonuclear reactions triggered by LWFA-accelerated beams, it will require beam energies with a few tens of MeV [16, 17], which is the goal of Development Phase 2. However, theoretical investigation on this subject is being performed with aid of IPEN Nuclear Engineering staff. Moreover, the recent approval of an experimental proposal submitted to the current edition of the LaserNetUS program will allow us to conduct this research in parallel with the development of our local SM-LWFA. Finally, despite its limitations, this initiative might become the seed of a national LWFA program.

ACKNOWLEDGEMENTS

The authors acknowledge the support of the funding agencies, FAPESP (Grant # 2018/25961), and CNPq and CAPES for scholarships and research grants. In addition, the authors acknowledge the LNCC for providing access to the Santos Dumont HPC system. Finally, the authors thank Prof. Dr. Sudeep Banerjee, from the University of Nebraska-Lincoln, for helpful discussions in setting up the experiment.

REFERENCES

- [1] T. Tajima and J. M. Dawson, "Laser Electron Accelerator", *Phys.Rev.Lett.*, vol. 43, no. 4, pp. 267–270, 1979. doi:10.1103/PhysRevLett.43.267
- [2] D. Strickland and G. Mourou, "Compression of amplified chirped optical pulses", *Opt. Commun.*, vol. 56, pp. 219–221, 1985. doi:10.1016/0030-4018(85)90120-8
- [3] G. P. Agrawal and N. A. Olsson, "Self-phase modulation and spectral broadening of optical pulses in semiconductor laser amplifiers", *IEEE J. Quantum Elec.*, vol. 25, pp. 2297–2306, 1989. doi:10.1109/3.42059.
- [4] M. Nisoli, "Compression of high-energy laser pulses below 5fs", *Opt. Lett.*, vol. 22, p. 522, 1997. doi:10.1364/OL.22.000522
- [5] A. J. Gonsalves *et al.*, "Petawatt Laser Guiding and Electron Beam Acceleration to 8 GeV in a Laser-Heated Capillary Discharge Waveguide", *Phys.Rev.Lett.*, vol. 122, no. 8, p. 084801, 2019. doi:10.1103/PhysRevLett.122.084801
- [6] E. Esarey, C. Schroeder, and W. P. Leemans, "Physics of laser-driven plasma-based electron accelerators", *Rev. Mod. Phys.*, vol. 81, no. 3, pp. 1229–1285, 2009. doi:10.1103/RevModPhys.81.1229
- [7] L. Rovige *et al.*, "Demonstration of stable long-term operation of a kilohertz laser-plasma accelerator", *Phys. Rev. Accel. Beams*, vol. 23, no. 9, p. 093401, 2020. doi:10.1103/PhysRevAccelBeams.23.093401
- [8] M. I. Santala *et al.*, "Observation of a hot high-current electron beam from a self-modulated laser wakefield accelerator", *Phys.Rev.Lett.*, vol. 86, no. 7, pp. 1227–1230, 2001. doi:10.1103/PhysRevLett.86.1227
- [9] R. E. Samad, S. L. Baldochi, G. E. C. Nogueira, and N. D. Vieira, "30 W Cr:LiSrAlF6 flashlamp-pumped pulsed laser", *Opt. Lett.*, vol. 32, pp. 50–52, 2007. doi:10.1364/OL.32.000050
- [10] R. E. Samad, G. E. C. Nogueira, S. L. Baldochi, and N. D. Vieira, "5 Hz flashlamp pumped Cr:LiSAF multipass amplifier for ultrashort pulses", *J. Opt. A: Pure Appl.*, vol. 10, p. 104010, 2008. doi:10.1088/1464-4258/10/10/104010
- [11] B. B. Chiomento *et al.*, "Development of dielectric de Laval nozzles for laser electron acceleration by ultrashort pulses micromachining", in *Proc. 2021 SBFoton International Optics and Photonics Conference (SBFoton IOPC)*, Campinas, Brazil, 31 May - 2 Jun. 2021.
- [12] R. E. Samad, A. V. F. Zuffi, E. P. Maldonado, and N. D. Vieira, "Development and Optical Characterization of Supersonic Gas Targets for High-Intensity Laser Plasma Studies", in *Proc. 2018 SBFoton International Optics and Photonics Conference (SBFoton IOPC)*, Campinas, Brazil 8–10 Oct. 2018.
- [13] F. B. D. Tabacow *et al.*, "Theoretical and experimental study of supersonic gas jet targets for laser wakefield acceleration", in *Proc. 2021 SBFoton International Optics and Photonics Conference (SBFoton IOPC)*, Campinas, Brazil 31 May - 2 Jun. 2021, unpublished.
- [14] A. V. F. Zuffi *et al.*, "Development of a modified Mach-Zehnder interferometer for time and space density measurements for laser wakefield acceleration", in *Proc. 2021 SBFoton International Optics and Photonics Conference (SBFoton IOPC)*, Campinas, Brazil, 31 May - 2 June 2021.
- [15] R. Lehe, M. Kirchen, I. A. Andriyash, B. B. Godfrey, and J. Vay, "A spectral, quasi-cylindrical and dispersion-free Particle-In-Cell algorithm", *Comput. Phys. Commun.*, vol. 203, pp. 66–82, 2016. doi:10.1016/j.cpc.2016.02.007
- [16] A. D. Roberts *et al.*, "Measured bremsstrahlung photonuclear production of ⁹⁹Mo (^{99m}Tc) with 34 MeV to 1.7 GeV electrons", *Appl. Radiat. Isot.*, vol. 96, pp. 122–128, 2014. doi:10.1016/j.apradiso.2014.11.008
- [17] Z. Sun, "Review: Production of nuclear medicine radioisotopes with ultra-intense lasers", *AIP Advances*, vol. 11, p. 040701, 2021. doi:10.1063/5.0042796